IOP Publishing New J. Phys. 17 (2015) 073010 doi:10.1088/1367-2630/17/7/073010

New Journal of Physics

The open access journal at the forefront of physics

Deutsche Physikalische Gesellschaft DPG

IOP Institute of Physics

Published in partnership with: Deutsche Physikalische Gesellschaft and the Institute of Physics

OPEN ACCESS

RECEIVED
6 March 2015

REVISED
14 May 2015

ACCEPTED FOR PUBLICATION
9 June 2015

PUBLISHED
9 July 2015

PAPER

Complex thermorheology of living cells

B U S Schmidt[1,2], T R Kießling[1], E Warmt, A W Fritsch, R Stange and J A Käs

Universität Leipzig, Faculty of Physics and Earth Sciences, Institute for Experimental Physics I, Linnéstraße 5, D-04103 Leipzig, Germany

[1] These author contributed equally to this work.

[2] Author to whom any correspondence should be addressed.

E-mail: sebastian.schmidt@uni-leipzig.de, tobias.kiessling@uni-leipzig.de, enrico.warmt@uni-leipzig.de, anatol.fritsch@uni-leipzig.de, stangeroll@googlemail.com and jkaes@physik.uni-leipzig.de

Keywords: biomechanics, thermorheology, cell rheology

Abstract

Temperature has a reliable and nearly instantaneous influence on mechanical responses of cells. As recently published, MCF-10A normal epithelial breast cells follow the time–temperature superposition (TTS) principle. Here, we measured thermorheological behaviour of eight common cell types within physiologically relevant temperatures and applied TTS to creep compliance curves. Our results showed that superposition is not universal and was seen in four of the eight investigated cell types. For the other cell types, transitions of thermorheological responses were observed at 36 °C. Activation energies (E_A) were calculated for all cell types and ranged between 50 and 150 kJ mol^{-1}. The scaling factors of the superposition of creep curves were used to group the cell lines into three categories. They were dependent on relaxation processes as well as structural composition of the cells in response to mechanical load and temperature increase. This study supports the view that temperature is a vital parameter for comparing cell rheological data and should be precisely controlled when designing experiments.

1. Introduction

Temperature is known to affect mechanical properties of any viscoelastic material. Without more information on the thermal dependence of the cells polymer structure and its related processes, we are limited in our deductions from rheological experiments. In 2013, time–temperature superposition (TTS) has been proposed to delineate creep compliance behaviour of MCF-10A breast epithelial cells [1]. While TTS is a well known concept in polymer physics, it was remarkable that cell deformation data can be matched to this model, considering that cells are a heterogeneous system composed of different structure proteins.

Thermal behaviour of cells is determined by two elementary parts: cytoplasm dominating with viscous contribution and cross-linked polymers forming a viscoelastic material [2]. Mechanical properties of cells and their responses to external forces as well as thermal variations are integral parts of cellular functions like embryogenesis, wound healing, cell division, and metastasis [3–6]. Cell rheology helps to describe dynamics and composition of the cytoskeleton as well as underlying molecular processes [7]. While rheological methods are common in cell biology [8], temperature impact has only recently been integrated in biomechanical cell studies or models [9–11]. For instance temperature sensitive ion channels have been found to govern response to heat and mechanical stress [12–14].

We hypothesized that the known model for TTS would be universal for all cell types and wanted to see if there are different types of behaviour. For a more diverse understanding of TTS, eight commonly used cell lines were examined at five different temperatures and their activation energies calculated.

2. Methods and materials

2.1. Thermorheological setup

An optical stretcher setup [15] was used to investigate mechanical deformations of single suspended cells from eight different cell lines at various temperatures. This setup has been previously described in detail, see [1, 16].

Briefly, cells were held in between two counter propagating laser beams ($\lambda = 1064$ nm). Due to applied laser power, cells experienced both an optical force pulling on the cell membrane ($\sigma \approx 10$ Pa peak stress [16]) and an increase in temperature caused by laser light absorption ($\Delta T_{\text{stretch}} \approx 25$ K W^{-1} [1, 17]). The applied laser power P_{stretch} can then be translated to an effective temperature:

$$T_{\text{eff}} = T_{\text{setup}} + \Delta T_{\text{stretch}} P_{\text{stretch}}. \tag{1}$$

The calibration from [1] was reused, i.e. the temperature sensitive dye rhodamine B (Sigma-Aldrich, USA) was flushed into the capillary channel and the temperature increase for six different powers measured via the intensity change. Wetzel *et al* reported a temperature increase of 21 ± 2 K after 0.5 s for an equilibrium temperature increase of 23 ± 2 K (for 1 W applied laser power) [18]. During the cell deformation measurement, the microscope and stage temperature T_{setup} was held at 11 °C. The step stress is applied for 2 s to the cell. Thus, during the stretch laser excitation, trapped cells were heated up to approximately 37 °C (T_{eff} between 28 and 44 °C).

All measurements were done in the same setup under similar conditions, providing best comparability. Cells were stretched by a randomly chosen stretch laser power between 680 and 1320 mW, and showed creep behaviour. Cell deformations were analysed afterwards by a self-written edge detection algorithm in Matlab (Mathworks, USA), explained in [15]. Since optically induced surface stress σ_0 increases linearly with the applied laser power [19, 20], the observed cellular deformation was directly translated into creep compliance $J(t)$:

$$J(t) = \frac{\varepsilon(t)}{\sigma_0}. \tag{2}$$

Assuming linear viscoelastic cellular response $\varepsilon(t)$. Creep experiments are described via:

$$J(t, T_{\text{ref}}) = \frac{J_{\text{i}}\left(t/a_{T_{\text{i}}}, T_{\text{i}}\right)}{b_{T_{\text{i}}}}. \tag{3}$$

Creep compliance J_{i} curves, measured at T_{i}, were plotted logarithmically and shifted to overlap at reference temperature T_{ref} (TTS), following [21]. Each curve J_{i} contained over 100 cells. For cell lines that behave thermorheologically simple, only a time shift factor $a_{T_{\text{i}}}$ is necessary. If the creep curves were scaled by an additional modulus shift factor $b_{T_{\text{i}}}$, cells were considered thermorheologically complex [22]. If $a_{T_{\text{i}}}$ shows a simple Arrhenius dependency [23]

$$\log(a_{T_{\text{i}}}) = \frac{E_{\text{A}}}{R}\left(\frac{1}{T} - \frac{1}{T_{\text{ref}}}\right), \tag{4}$$

it was possible to calculate a constant activation energy E_{A} (R is universal gas constant). Assuming that cells behave like glassy material [24–26], activation energy becomes temperature dependent near glass transition temperature T_{g} and $a_{T_{\text{i}}}$ above T_{g} is often represented by the William–Landel–Ferry equation [22, 23]:

$$\log(a_{T_{\text{i}}}) = \frac{-C_1(T_{\text{i}} - T_{\text{ref}})}{C_2 + (T_{\text{i}} - T_{\text{ref}})}, \tag{5}$$

with C_1 and C_2 as empirical parameters. Master curves were constructed from creep compliance curves J_{i} via a custom-made algorithm. A reference temperature was selected as $T_{\text{ref}} = 36$ °C and all other curves were scaled according equation (3). $a_{T_{\text{i}}}$ and $b_{T_{\text{i}}}$ were determined using least squares fitting minimizing the χ^2 value. Bootstrapping was used to establish the 95% confidence interval of the mean of the deformation curves. When it was possible to overlay these bounds, the fit was deemed acceptable. The errors for $a_{T_{\text{i}}}$ and $b_{T_{\text{i}}}$ were estimated with the maximum distance to the confidence bounds.

2.2. Cell culture

All cell lines except keratinocytes were cultured in humid atmosphere at 37 °C with 5% CO_2.

MCF-10A cell line (CRL-10317) was maintained in a 1:1 mixture of Dulbecco's modified Eagle medium/Ham's F12 with L-glutamine (E15-813, PAA) supplemented with 5% horse serum (A15-151, PAA), 20 ng ml^{-1} epidermal growth factor, 10 μg ml^{-1} insulin (I6634, Sigma-Aldrich), 100 ng ml^{-1} cholera toxin, 500 ng ml^{-1} hydrocortisone and 100 U ml^{-1} penicillin/streptomycin.

MCF-7 cell line was maintained in minimum essential medium (E15-024, PAA) supplemented with 10% fetal calf serum (A15-043, PAA), 1% non-essential amino acids, 0.5% bovine insulin stock solution dissolved at 2 mg ml^{-1} in diluted HCl (pH 2–3), 10 μg ml^{-1} insulin (I6634, Sigma-Aldrich), 110 μg ml^{-1} sodium pyruvate (P5280, Sigma-Aldrich) and 100 U ml^{-1} penicillin/streptomycin.

MDA-MB-436 and MDA-MB-231 cell line were maintained in Dulbecco's modified Eagle medium supplemented with 10% calf serum, and 100 U ml^{-1} penicillin/streptomycin.

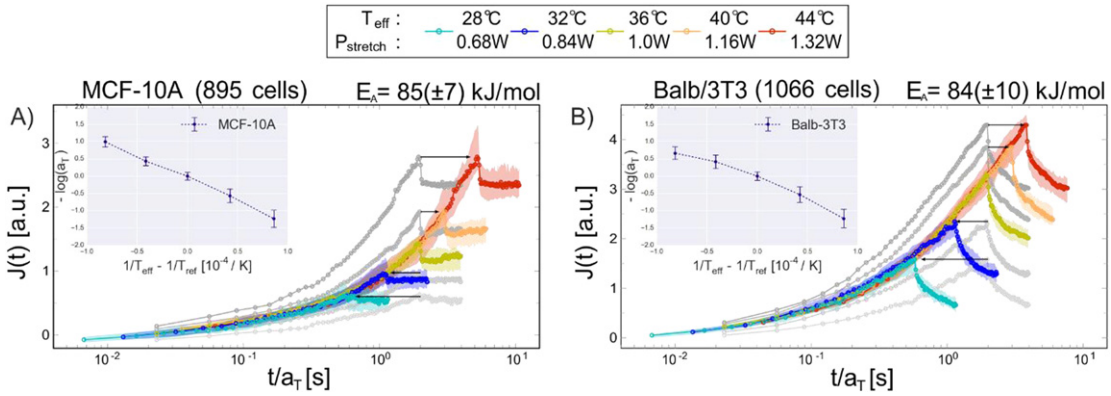

Figure 1. Creep compliance curves of MCF-10A (A) and Balb/3T3 (B). Both cell types show thermorheologically simple behaviour. Cellular creep response is plotted logarithmically for five different laser powers (grey curves). Coloured curves are scaled to overlap via time shift factor a_T, indicated by arrows. Modulus shift b_T is kept constant to one and is not needed for scaling. Insets show Arrhenius dependency of a_T. Stretch powers $P_{stretch}$ and corresponding temperature during stretch T_{eff} are colour-coded. Activation energies of both cell types are approximately 85 kJ mol^{-1}.

Chinese hamster ovarian CHO-K1 cell line was maintained in ATCC-formulated F-12K medium supplemented with 10% fetal bovine serum.

Balb/3T3 clone A31 mouse fibroblast cell line and SV-T2 transformed mouse fibroblast cell line were maintained in Dulbecco's modified Eagle medium supplemented with 10% calf serum, 1% 1 M HEPES (H4034, Sigma-Aldrich) and 100 U ml^{-1} penicillin/streptomycin.

Mouse keratinocytes were derived from strain C57Bl6 on 3T3J2 feeders and spontaneously immortalized. Cells were maintained at 32 °C with 5% CO_2 in Dulbecco's modified Eagle medium/Ham's F12 low calcium (F-9092, Biochrom) supplemented with 10% (v/v), 10% Chelex 100 treated fetal calf serum (A15-151, PAA), 0.18 mM adenine, 0.5 μg mL^{-1} hydrocortisone, 5 μg mL^{-1} insulin, 100 pM cholera toxin (all Sigma-Aldrich), 10 ng mL^{-1} EGF, 100 U mL^{-1} sodium pyruvate, 100 μg mL^{-1} penicillin/streptomycin, and 2 mM glutamax (all Invitrogen).

For all measurements, cells were detached with 0.025% (w/v) trypsin-EDTA in PBS, resuspended in ~10 ml medium and centrifuged at 100 g for 4 min. Medium was aspirated off and cell pellets were suspended in ~1 ml medium for a measurement concentration of $\sim 5 \times 10^6$ cells/ml. Cells were from a single culture flask for each experiment to exclude differences in passage number or culturing time.

3. Results and discussion

Eight different cell types were stretched by five different laser powers. Thermorheologically simple behaviour could not be observed for every cell line. Balb/3T3 and MCF-10A exhibited simple behaviour, i.e. the creep curves were shifted horizontally only via the time shift factor a_T, as seen in figure 1. All values for a_T and b_T are given in the appendix: data tables A1 and A2.

Cells exhibit an increase of compliance at higher temperatures caused by a loss of viscosity due to increased temperature. This indicates that temperature change is the main independent variable affecting viscosity of these cell lines. Plotting the time shift factors a_T over $T_i - T_{ref}$, as is usual for dense polymer solutions of high molecular weight at temperatures near glass transition [27, 28], reveals linear dependency. Thus, the Arrhenius equation (4) is sufficient to describe the observed dependency of a_T around $T_{eff} = 37$ °C and provides a value for the activation energy (E_A). With $T_{ref} = 36$ °C, the activation energy of MCF-10A cells is $E_A = 85$ kJ mol^{-1} and of Balb/3T3 cells is $E_A = 84$ kJ mol^{-1}. Both cell types, originating from different tissues, have a similar and linear sensitivity to temperature.

MCF-7 cells (figures 2(A) and (C)) behaved simply except at $T_{eff} = 44$ °C, where additional vertical scaling via modulus shift factor b_T was necessary for superposition. Stiffening over a certain temperature threshold had been previously observed for the MCF-10A cells in Kießling *et al* [1]. Due to the short timescales of the temperature change in our experiments, a scaling of b_T implied instant structural transformation of the cytoskeleton or other intracellular structures e.g. the cell's nucleus. MCF-7 nuclei are known to contract in the optical stretcher around $T_{eff} = 45$ °C [11]. Due to cross-links of structure proteins, this contraction affects the whole cell, which appears here to stiffen the cell requiring an additional scaling via b_T. With an activation energy of $E_A = 142$ kJ mol^{-1}, MCF-7 cells have the highest sensitivity to temperature.

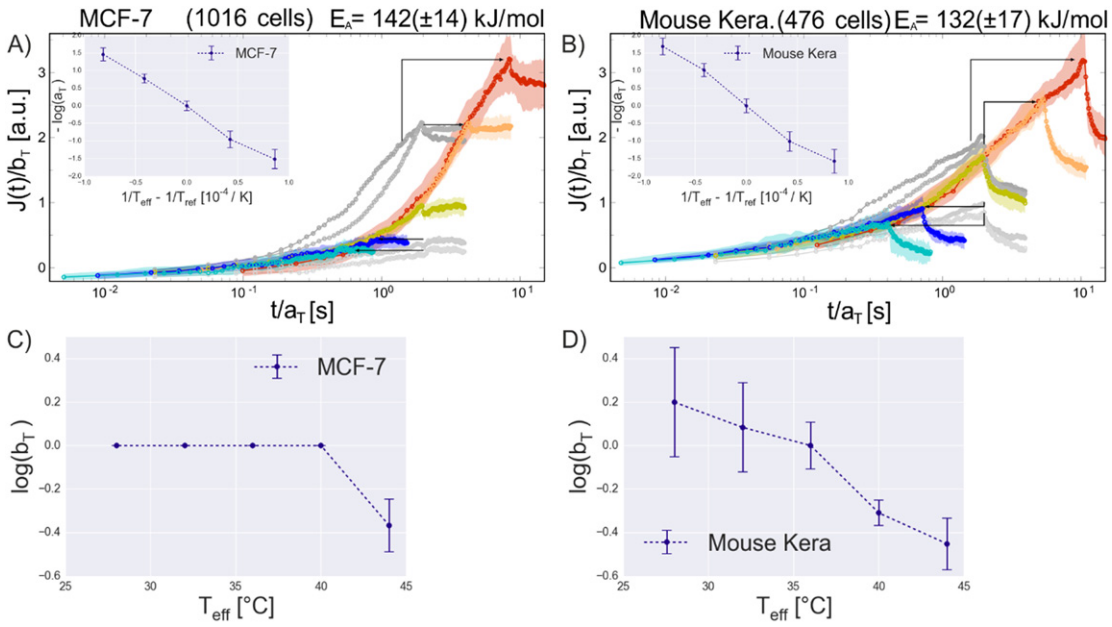

Figure 2. MCF-7 (A) cells and keratinocytes (B) are superposed with additional scaling via b_T, see (C) and (D), indicating thermorheologically complex behaviour. Coloured curves are scaled to overlap horizontally via a_T (see insets), and vertically via b_T. Activation energies of both cell types are similar around 140 kJ mol^{-1}.

Keratinocytes (figures 2(B) and (D)) behave similar to MCF-7 cells, i.e. their curves do not match just by scaling with a_T. Therefore, all creep curves need to be additionally adapted via b_T to overlap properly. Again, b_T decreases for higher temperatures, suggesting changes in elasticity-contributing structures for these short time scales and entropic mechanisms. Since the experiments were conducted around approximately $T_{eff} \approx 37$ °C, massive protein denaturing is unlikely. The activation energy for keratinocytes was $E_A = 132$ kJ mol^{-1} .

Creep curves of the other four cell lines—CHO-K1, MDA-MB-231, MDA-MB-436, and SV-T2—did not overlap to form a master curve, even when incorporating both scaling factors, as shown in figure 3. Curve shapes did not allow superposition via equation (3). However they were scaled by a_T, to overlap during the beginning of the stretch, since the temperature influence is shorter. Activation energies were calculated from chosen scaling, but did not have the same meaning considering that they did not form a master curve. A quantification of the impact of temperature in terms of TTS (3) is only significant when curves superpose.

For lower (28 and 32 °C) and for higher temperatures (40 and 44 °C) overlapping curves via scaling was achieved, i.e. turquoise and blue curves overlap best and respectively orange and red curves. At approximately $T_{eff} = 36$ °C a transition of creep behaviour occurred. This could be indicative for a fundamental change in dominating relaxation processes between deformations at lower and higher temperatures. In that sense, thermorheological measurements could evolve to a powerful tool for the identification of main-load bearing structures in cells and for discerning their contribution to the mechanical properties on a whole cell level.

An artefact of the chosen scaling is that creep curves of higher temperatures deviate from curves at lower temperatures by becoming more compliant. For MDA-MB-231, MDA-MB-436, CHO-K1, and SV-T2 cells weakening or even bound breaking processes or other structural alterations leading to more compliance might occur within the cells during heating. This is contrary to the superposing cell lines. The 44 °C curve of MCF-7, for example, would appear less compliant, if it were scaled just with a_T and overlap at the beginning of the stretch. Thus, different temperature dependent molecular mechanisms might play a role in cytoskeletal assembly. Further detailed investigations need to be conducted in order to resolve the exact underlying mechanisms of differences in relevant load bearing structures leading to cellular softening or stiffening in different cell types.

Considering the stepwise temperature increase in conjunction with the applied step-stress, it is not trivial to apply an appropriate model to reflect the observed creep functions. The presented significant changes in thermorheological behaviour are visible by constructing the master curve during TTS. The advantage of TTS is that no assumptions of an explicit functional form of a creep compliance are necessary. The only assumptions are viscoelastic linearity and the validity of the main statement of TTS i.e. that temperature causes a rescaling of the time and the modulus axes.

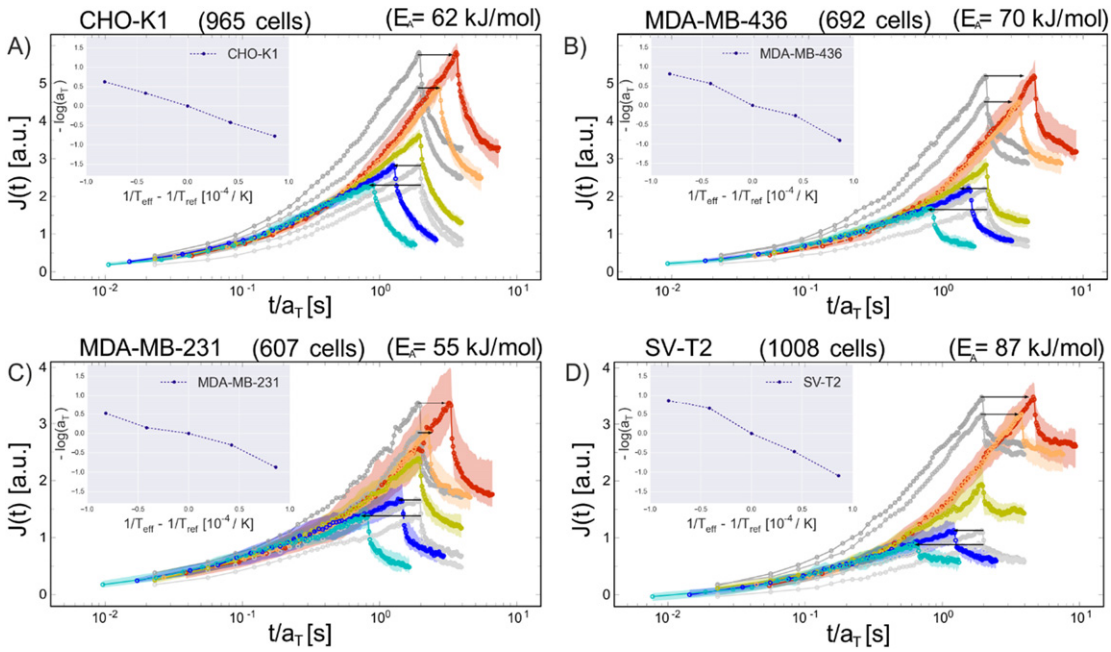

Figure 3. CHO-K1 (A), MDA-MB436 (B), MDA-MB231 (C) and SV-T2 (D) were not superimposable via TTS. Coloured curves are scaled to overlap at least at the beginning of the applied stress. Curves are scaled via a_T (see insets) to superpose for lower temperatures (turquoise and blue) and higher temperatures (orange and red), respectively, and are separated by a transition regime around $T_{eff} = 36$ °C. Activation energies are shown in brackets. They represent the value resulting from the chosen scaling while not being constant activation energies.

Cells are a complex compound of different polymers and TTS can be applied on a whole cell level. This would classify cellular matter as being a truly emergent material, in which the temperature dependencies of relaxation processes of the single components have merged into a single compound value. Cell types with no thermorheologically simple behaviour may have lower connectivity of cytoskeletal components. Different individual thermal properties of structural elements change their contribution towards the creep curve, making adaption by the modulus shift factor b_T necessary.

Glass transition might be another explanation for application of TTS, assuming only one thermally activated process dominates cellular response. With respect to the glassy character of cellular matter [24, 25], one of the components may undergo a glass transition. During optical stretching, the cells experience an instant heating leading to a drop of viscosity within the cell. The effect of heating on cell mechanics results in an increased deformability of about 10% per Kelvin. With regard to heating and instantaneous loss of viscosity during optical stretcher measurements, cells reveal a linear mechanical cell response to the applied optical force.

There are no comparative studies for thermal effects in single cells, fitting our time scale. However, qualitatively similar results for adherent cells on longer time scales have been reported [10].

In this study, we focused on physical properties and passive responses of cells rather than on biological alterations. Biological adaption processes during stretching may be excluded, since we only investigated short time responses, up to few seconds. Altered protein expression and delayed structural conversions in polymer networks (e.g. cytoskeleton) during heating need much more time, about minutes and hours [29]. Future work might involve specific up or down regulation of cytoskeleton contributors. Especially the actin cortex is often dominating the mechanical response [30, 31]. Here, it has to be taken into account that there are differences between suspended cells and adherent cells that may lead to contradicting results using cytoskeleton-altering drugs. For instance stress fibers in adherent cells have an impact [26] and myosin II activity in suspended cells [32].

We propose single and complex thermorheology as a powerful approach for cell-rheological studies. Differences in the applicability of TTS provide deeper insight in cell mechanics, since no assumptions about an underlying model concerning material functions are necessary. The results demonstrate that the deformability of living cells strongly depends on temperature and differs qualitatively between various cell types.

4. Conclusions

Temperature variations significantly affect mechanical properties of cells. Deformation changes of approximately 10% per degree Kelvin were observed for all cell lines, which was consistent with a drop in

viscosity. Comparisons of cell lines show that thermorheologically simple behaviour is not universal in cells, but has been observed in certain cell types. Superposition of creep curves was not achieved for half of the cell lines due to nonlinear temperature dependence of intracellular processes and structural relaxation times. Scaling factors and comparison of creep curves provides valuable information about deformation processes in response to applied forces. Different characteristics of curves are related to composition and structure of the cytoskeleton providing more insight to the complex cellular assembly. Based on these finding we suggest incorporating temperature as a vital parameter when comparing cell rheology studies or for the design of future experiments.

Acknowledgments

Graduate student Sebastian Schmidt (Project KA1116/7-1) was financed by the DFG. We thank Jörg Schnauß for helpful discussions. Financial support was provided by the Deutsche Forschungsgemeinschaft within the Graduate School BuildMoNa, the European structural funds ESF and the Sächsische Aufbau Bank SAB. We acknowledge support from the German Research Foundation (DFG) and Universität Leipzig within the program of Open Access Publishing.

Appendix. Data tables

Tables A1–A8 contain employed scaling factors a_T and b_T for each cell line.

Table A1. Scaling factors for MCF-10.

$P_{stretch}$	T_{eff}	a_T	± Error a_T	b_T
1.32 W	44 °C	0.3714	0.06	1
1.16 W	40 °C	0.6505	0.09	1
1.00 W	36 °C	1.0	0.12	1
0.84 W	32 °C	1.7634	0.38	1
0.68 W	28 °C	3.4272	0.97	1

Table A2. Scaling factors for Balb/3T3.

$P_{stretch}$	T_{eff}	a_T	± Error a_T	b_T
1.32 W	44 °C	0.5150	0.10	1
1.16 W	40 °C	0.6590	0.14	1
1.00 W	36 °C	1.0	0.13	1
0.84 W	32 °C	1.7061	0.43	1
0.68 W	28 °C	3.4070	1.02	1

Table A3. Scaling factors for MCF-7.

$P_{stretch}$	T_{eff}	a_T	± Error a_T	b_T	± Error b_T
1.32 W	44 °C	0.2321	0.05	0.6923	0.09
1.16 W	40 °C	0.4602	0.06	1	0.00
1.00 W	36 °C	1.0	0.15	1	0.00
0.84 W	32 °C	2.5842	0.69	1	0.00
0.68 W	28 °C	4.5378	1.44	1	0.00

Table A4. Scaling factors for keratinocytes.

$P_{stretch}$	T_{eff}	a_T	± Error a_T	b_T	± Error B_T
1.32 W	44 °C	0.1848	0.05	0.6367	0.08
1.16 W	40 °C	0.3622	0.07	0.7338	0.04
1.00 W	36 °C	1.0	0.22	1	0.11
0.84 W	32 °C	2.7436	0.87	1.0877	0.25
0.68 W	28 °C	4.8236	1.93	1.2210	0.35

Table A5. Scaling factors for CHO-K1.

$P_{stretch}$	T_{eff}	a_T	b_T
1.32 W	44 °C	0.5356	1
1.16 W	40 °C	0.7170	1
1.00 W	36 °C	1.0	1
0.84 W	32 °C	1.5302	1
0.68 W	28 °C	2.1767	1

Table A6. Scaling factors for MDA-MB-436.

$P_{stretch}$	T_{eff}	a_T	b_T
1.32 W	44 °C	0.4425	1
1.16 W	40 °C	0.5679	1
1.00 W	36 °C	1.0	1
0.84 W	32 °C	1.3050	1
0.68 W	28 °C	2.4559	1

Table A7. Scaling factors for MDA-MB-231.

$P_{stretch}$	T_{eff}	a_T	b_T
1.32 W	44 °C	0.5940	1
1.16 W	40 °C	0.8616	1
1.00 W	36 °C	1.0	1
0.84 W	32 °C	1.3466	1
0.68 W	28 °C	2.3971	1

Table A8. Scaling factors for SV-T2.

$P_{stretch}$	T_{eff}	a_T	b_T
1.32 W	44 °C	0.4210	1
1.16 W	40 °C	0.5206	1
1.00 W	36 °C	1.0	1
0.84 W	32 °C	1.6007	1
0.68 W	28 °C	2.9824	1

References

[1] Kießling T R, Stange R, Käs J A and Fritsch A W 2013 Thermorheology of living cells—impact of temperature variations on cell mechanics *New J. Phys.* **15** 045026

[2] Kasza K E, Rowat A C, Liu J, Angelini T E, Brangwynne C P, Koenderink G H and Weitz D A 2007 The cell as a material *Curr. Opin. Cell Biol.* **19** 101–7

[3] Huber F, Schnauß J, Rönicke S, Rauch P, Müller K, Fütterer C and Käs J 2013 Emergent complexity of the cytoskeleton: from single filaments to tissue *Adv. Phys.* **62** 1–112

[4] McKinnell R G and Tarin D 1984 Temperature-dependent metastasis of the Lucke renal carcinoma and its significance for studies on mechanisms of metastasis *Cancer Metastasis Rev.* **3** 373–86

[5] Lepock J R 2003 Cellular effects of hyperthermia: relevance to the minimum dose for thermal damage *Int. J. Hyperthermia* **19** 252–66

[6] Ream R A, Theriot J A and Somero G N 2003 Influences of thermal acclimation and acute temperature change on the motility of epithelial wound-healing cells (keratocytes) of tropical, temperate and Antarctic fish *J. Exp. Biol.* **206** 4539–51

[7] Seltmann K, Fritsch A W, Käs J A and Magin T M 2013 Keratins significantly contribute to cell stiffness and impact invasive behavior *Proc. Natl Acad. Sci. USA* **110** 18507

[8] Suresh S 2007 Biomechanics and biophysics of cancer cells *Acta Biomater.* **3** 413–38

[9] Rico F, Chu C, Abdulreda M H, Qin Y and Moy V T 2010 Temperature modulation of integrin-mediated cell adhesion *Biophys. J.* **99** 1387–96

[10] Sunyer R, Trepat X, Fredberg J J, Farré R and Navajas D 2009 The temperature dependence of cell mechanics measured by atomic force microscopy *Phys. Biol.* **6** 025009

[11] Warmt E, Kießling T R, Stange R, Fritsch A W, Zink M and Käs J A 2014 Thermal instability of cell nuclei *New J. Phys.* **16** 073009

[12] Gyger M, Stange R, Kießling T R, Fritsch A, Kostelnik K B, Beck-Sickinger A G, Zink M and Käs J A 2014 Active contractions in single suspended epithelial cells *Eur. Biophys. J.* **43** 11–23

[13] Gyger M, Rose D, Stange R, Kießling T, Zink M, Fabry B and Käs J A 2011 Calcium imaging in the optical stretcher *Opt. Express* **19** 19212–22
[14] Chan C J, Whyte G, Boyde L, Salbreux G and Guck J 2014 Impact of heating on passive and active biomechanics of suspended cells *Interface Focus* **4** 20130069
[15] Lincoln B, Schinkinger S, Travis K, Wottawah F, Ebert S, Sauer F and Guck J 2007 Reconfigurable microfluidic integration of a dual-beam laser trap with biomedical applications *Biomed. Microdevices* **9** 703–10
[16] Guck J, Ananthakrishnan R, Mahmood H, Moon T J, Cunningham C C and Käs J 2001 The optical stretcher: a novel laser tool to micromanipulate cells *Biophys. J.* **81** 767–84
[17] Ebert S, Travis K, Lincoln B and Guck J 2007 Fluorescence ratio thermometry in a microfluidic dual-beam laser trap *Opt. Express* **15** 15493–9
[18] Wetzel F, Rönicke S, Müller K, Gyger M, Rose D, Zink M and Käs J 2011 Single cell viability and impact of heating by laser absorption *Eur. Biophys. J.* **40** 1109–14
[19] Guck J, Ananthakrishnan R, Moon T J, Cunningham C C and Käs J 2000 Optical deformability of soft biological dielectrics *Phys. Rev. Lett.* **84** 5451–4
[20] Guck J *et al* 2005 Optical deformability as an inherent cell marker for testing malignant transformation and metastatic competence *Biophys. J.* **88** 3689–98
[21] Luo W B, Wang C H and Zhao R G 2007 Application of time–temperature–stress superposition principle to nonlinear creep of poly(methyl methacrylate) *Key Eng. Mater.* **340-1** 1091–6
[22] Schwarzl F and Staverman A J 1952 Time-temperature dependence of linear viscoelastic behavior *J. Appl. Phys.* **23** 838–43
[23] Ferry J D 1980 *Viscoelastic Properties of Polymers* (New York: Wiley)
[24] Trepat X, Deng L, An S S, Navajas D, Tschumperlin D J, Gerthoffer W T, Butler J P and Fredberg J J 2007 Universal physical responses to stretch in the living cell *Nature* **447** 592–5
[25] Fabry B, Maksym G N, Butler J P, Glogauer M, Navajas D and Fredberg J J 2001 Scaling the microrheology of living cells *Phys. Rev. Lett.* **87** 148102
[26] Maloney J M, Nikova D, Lautenschläger F, Clarke E, Langer R, Guck J and Van Vliet K J 2010 Mesenchymal stem cell mechanics from the attached to the suspended state *Biophys. J.* **99** 2479–87
[27] Williams M L, Landel R F and Ferry J D 1955 The temperature dependence of relaxation mechanisms in amorphous polymers and other glass-forming liquids *J. Am. Chem. Soc.* **77** 3701–7
[28] Wood-Adams P and Costeux S 2001 Thermorheological behavior of polyethylene: effects of microstructure and long chain branching *Macromolecules* **34** 6281–90
[29] Digel I, Kayser P and Artmann G M 2008 Molecular processes in biological thermosensation *J. Biophys.* **2008** e602870
[30] Salbreux G, Charras G and Paluch E 2012 Actin cortex mechanics and cellular morphogenesis *Trends Cell Biol.* **22** 536–45
[31] Cuvelier D, Théry M, Chu Y-S, Dufour S, Thiéry J-P, Bornens M, Nassoy P and Mahadevan L 2007 The universal dynamics of cell spreading *Curr. Biol.* **17** 694–9
[32] Chan C J, Ekpenyong A E, Golfier S, Li W, Chalut K J, Otto O, Elgeti J, Guck J and Lautenschläger F 2015 Myosin II activity softens cells in suspension *Biophys. J.* **108** 1856–69